

Hump formation mechanism in gas-jet-assisted keyhole laser welding of HR-2 stainless steel *

Shen Xianfeng, Teng Wenhua and Xu Chao

沈显峰, 滕文华, 许超 **

Abstract Gas-jet-assisted keyhole laser welding offers the possibility of a breakthrough in the limitations of penetration depth in laser welding, which currently suffers from equipment restrictions. A gas jet of sufficient intensity to assist the keyhole should be used to obtain suppressed plasma, a deepened keyhole, and increased penetration depth. However, an excessively strong gas jet gives rise to humps. The incident angle of the keyhole-assisted gas jet is 60° , with a nozzle ahead of the laser beam. A series of experiments were carried out with different welding velocities and gas parameters by using HR-2 hydrogen-resistant stainless steel and a slab CO_2 continuous-wave laser welding machine. The weld profiles can be categorized into four types, welds of traditional laser welding, welds of enhanced laser welding, undercut welds, and humping welds with increased gas pressure. A high-speed camera was employed in the experiments to monitor the formation of humps under an excessively strong gas jet. The results of analysis show that hump formation can be divided into six stages. Its main driving force is the intense turbulence of gas jet. There are two main reasons for hump formation: premature solidification of the molten pool caused by the large temperature gradient between the front and rear parts of the molten pool, and the emergence of a thin layer liquid bridge with one-directional flow under the enhanced cooling effect of excessively strong gas.

Key words gas-jet-assisted keyhole laser welding, hump formation mechanism, penetration depth, hydrogen-resistance stainless steel

0 Introduction

Welding is employed extensively for the manufacture of many thick-walled components in large ships^[1], nuclear power plant construction^[2], aerospace^[3-5], and other industries with requirements for increased penetration and low-distortion joints. Laser welding is characterized by high energy density, low heat input, large depth-to-width ratio, small heat-affected zone (HAZ), and other advantages, making it known as one of the most advanced welding techniques^[1,5]. With the development of new diode-pumped solid-state lasers, fiber lasers, and other new laser concepts, the scope and application of laser welding is expanding in the areas of automotive manufacturing, shipbuilding, aerospace engineering, machinery, and elec-

tronic instruments. However, the penetration depth of laser welding is restricted by the capability of the laser processing machine, which greatly limits its widespread application to thick-walled components. To overcome this limitation, researchers worldwide have obtained some practical methods including the laser-arc hybrid welding method^[3-4], active laser welding^[6], multipasses and multilayer laser welding with filler wire^[2]. Gas-jet-assisted laser welding is a method to achieve increased penetration depth^[7] where a gas jet is introduced at the blow keyhole to deepen the keyhole. Gas-jet-assisted keyhole laser welding is an enhanced laser welding technique to improve the penetration depth of laser welding without replacing a laser processing machine. However, the keyhole-assisted

* This work was supported by the National Natural Science Foundation of China (Grant No. 51005219) and the Key Project of Development Foundation of China Academy of Engineering Physics (Grant No. 2013A0203008).

** Shen Xianfeng, Teng Wenhua and Xu Chao, Institute of Machinery Manufacturing Technology, China Academy of Engineering Physics, Mianyang 621900. Shen Xianfeng, Corresponding author, E-mail: xianfeng_shen@163.com

gas jet pressure should be selected carefully because a weak gas jet cannot obtain the target result of a suppressed plasma, deepened keyhole, increased penetration depth, and an excessively strong gas jet causes the occurrence of humps.

The humping phenomenon is likely to occur during high-speed seam welding, which is likewise observed in arc, electron beam, and laser beam welding^[8-11]. Hump welds can be classified in two typical forms: gouging region morphology (GRM) and beaded for cylinder morphology (BCM)^[10]. Many previous studies have been performed for exploring the formation mechanism in high-speed welding and several models were proposed using the principles of liquid volume conservation including the surface tension gradient model^[11], arc-induced model, and liquid column instability model based on Rayleigh's theory^[12]. These models are highly targeted and each one is very effective in explaining a particular phenomenon, but there is no commonly accepted formation mechanism. Humping phenomenon in gas-jet-assisted keyhole laser welding is different from those in high-speed welding in which the hump weld may occur with the same welding speed and disproportionately high gas pressure. Some works have been focused on the plasma/metal vapor and the surrounding molten pool^[13-14], but their physical mechanism of humping has not been fully understood. In this paper, a series of experiments were carried out to investigate the effects of the keyhole-assisted gas on the welding results. A high-speed camera was employed in the experiments to monitor hump formation under the excessively intense gas jet. A six-stage hump formation mechanism is proposed to explain the process. Furthermore, the effects of the keyhole-assisted gas parameters on welding results and increase of penetration depth were also investigated.

1 Principle of gas-jet-assisted keyhole laser welding

The formation and maintenance of the keyhole is an essential physical phenomenon of deep penetration laser welding. Furthermore, it is theoretically feasible and practical to obtain enhanced keyhole and increased penetration by adding extra energy fields such as a magnetic field or by using external media such as ultrasonic vibrations and

gases. An effective approach is the use of keyhole-assisted gas. A sketch of gas-jet-assisted keyhole laser welding is illustrated in Fig. 1. The keyhole-assisted gas jet nozzle is typically installed very close to the keyhole position with a much higher pressure and smaller affected area, which cannot properly protect the molten pool area. Therefore, shielding gas is also needed in this processing; this can be introduced by one of two separate nozzles or the outer layer of a double-layer nozzle. In the layout of two separated nozzles shown in Fig. 1, keyhole-assisted gas jet could be mounted forwards or rearwards. The shielding gas nozzle with a larger diameter and lower pressure is mounted at a greater distance than the keyhole-assisted gas nozzle to minimize the possibility of turbulence generated by the two types of gases. The target location of keyhole-assisted gas shown in Fig. 1 is the keyhole center, while that of the shielding gas for protecting molten pool from oxidation is at a certain distance behind the keyhole.

2 Experiments

HR-2 stainless steel, whose chemical composition is shown in Table 1, was used in the experiments. The dimensions of the workpieces were 200 mm × 90 mm × 10 mm.

A CO₂ continuous-wave laser DC015, with a maximum power of 1.5 kW, was used to perform bead-on-plate welding in the experiments. The laser beam was focused on the workpiece surface by means of a focusing lens with a 150 mm focal length and the diameter of the focal spot was 0.4 mm. The keyhole-assisted gas jet nozzle of 1 mm diameter was mounted ahead of the welding direction with an incident angle θ of around 60° and nozzle height of 2 mm. An argon jet was used as the shielding gas with a pressure of 0.01 MPa and 3.8 mm nozzle diameter, incident angle γ of around 45°, and nozzle height 25 mm. A monochrome high-speed camera (Model: CL600X2) capable of a speed of 500 frames per second at its full resolution of 1 024 × 1 024 and an even higher speed at a lower resolution was used to monitor the welding process. A fiber laser with a wavelength of 808 nm and a maximum output power of 30 W was employed as an illumination source to obtain the desired images of the molten pool.

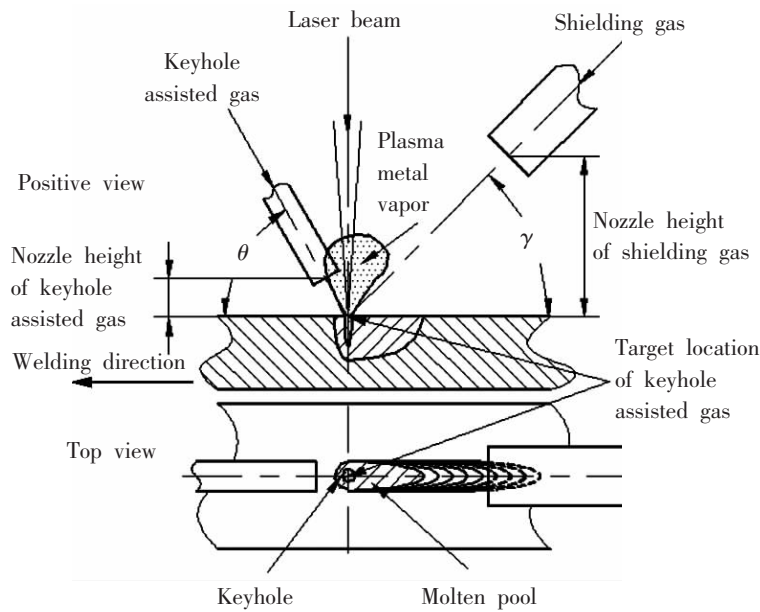


Fig. 1 Sketch of gas-jet-assisted keyhole laser welding

Table. 1 Chemical composition of HR-2 (wt. %)

C	Mn	Si	P	S	Cr	Ni	N	Fe
≤0.045	8.0 – 10.0	≤1.0	≤0.035	≤0.015	19.0 – 21.5	5.5 – 8.0	0.2 – 0.36	Balance

3 Results and discussion

3.1 Classification of welding effects according to keyhole-assisted gas-flow rate

The influences of the gas-flow rate of keyhole-assisted gas on the penetration depth and weld profile were investigated with changes of the keyhole-assisted argon gas-flow rate. The results, which include surface and cross-section morphology, are shown in Fig. 2. According to the welding profile, the welding results can be divided into four types: traditional laser welding, enhanced laser welding, undercut welding, and hump welding with an increased gas-flow rate.

Traditional laser welding zone (I): a goblet shape was obtained without keyhole-assisted gas.

Enhanced laser welding zone (II, III, IV): by using a suitable flow rate of keyhole-assisted gas, an increase in the penetration depth is obtained to a certain extent with a good weld and no undercut or underfill. Sample III has almost the same penetration depth as sample I. However,

sample III has a very different weld shape, in that its penetration width becomes wider at the bottom and middle welds, while becoming narrower at the top weld. It can be inferred that the keyhole shape with the keyhole-assisted gas has changed, more plasma is pressed into the keyhole, and the liquid metal is strongly expelled rearwards for the gas jet greatly changes the hydrodynamic melt flow^[13]. The penetration depth does not show a monotonically rising trend with an increase of the gas-flow rate, which is a result of the complex interaction between keyhole-assisted gas and plasma. This interaction leads to a non-monotonic change of keyhole shape and depth, which results in corresponding changes in the weld shape. Therefore, the spatial distribution of the keyhole-assisted gas-flow needs to match the laser power, welding speed, and other parameters of laser welding to achieve the desired penetration increase.

Undercut zone (V): the undercut phenomenon occurs by the side of the weld with a further increase of gas-flow rate and a higher cooling rate. The undercut occurs a-

long the weld toe in welded joints where base metal is melted and not fully covered by the deposited metal^[8, 15]. Undercut in gas-jet-assisted keyhole laser welding is generated owing to an overly strong gas-flow, resulting in sinking around the keyhole and formation of bumps at the rear of the keyhole, caused by inward melt flow toward the internal molten pool along the weld toe and poor wettability. This means that the undercut is driven by the surface ten-

sion force at the junction point of the solid, liquid and gas phases in the weld pool edge. Moreover, the greater inward melt flows, the higher is the possibility of undercut formation. Undercut is a more serious surface defect and should be avoided in welding because it can cause stress concentration and severe weld cracking. In gas-jet-assisted keyhole laser welding, a suitable gas-flow rate is essential to avoid undercuts.

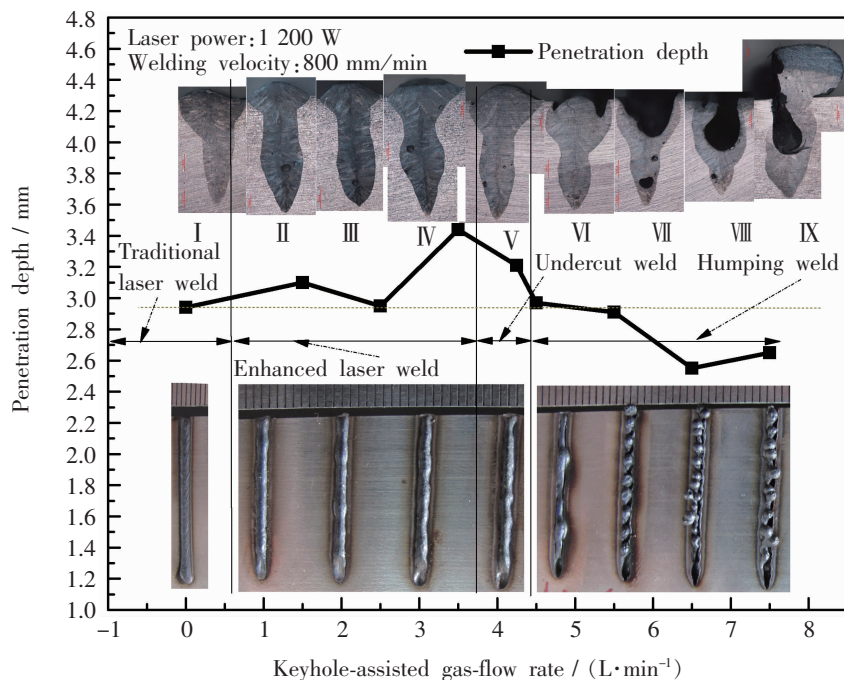


Fig. 2 Effects of keyhole-assisted gas-flow rate on penetration depth and weld profile

Humping weld zone (VI, VII, VIII, IX): with the gas-flow rate increasing and then enhanced cooling effect of keyhole assisted gas, the following weld beads gradually emerge: longer interval hump bead (presence of undercut), shorter interval hump bead (entrapped pores at the bottom of the weld), and cutting-like deep groove weld. It may also be seen from Fig.2 that the penetration depth does not increase, but decreases, with the increase in gas-flow rate. This is due to an excessively strong gas stream blowing liquid metal away from the keyhole, and too little liquid metal leads to a shallower keyhole, even a collapsed keyhole, which thus decreases the penetration depth.

Classification of four types of welding effects is of help in gaining a fuller understanding of the role of key-

hole-assisted gas flows.

3.2 Hump bead formation

Based on the high-speed images of the humping weld process, hump bead formation can be divided into the following steps in gas-jet-assisted keyhole laser welding: (a) Formation of a liquid molten pool generated by the laser; (b) Severe surface distortion of the molten pool and backward flow in the molten pool; excessive gas flow leads to excessive sinking of the molten pool, and drives the molten metal around keyhole to flow towards the tail of the molten pool. (c) Fluidity of the molten metal is reduced by the cold weld bead, and thus, a metal droplet emerges in the tail pool and the thin-layer liquid bridge in the cen-

tral pool. (d) The metal droplets grow with the continuous rearward flow of molten metal from the head of the molten pool to the tail through the thin-layer liquid bridge. (e) With the weld moving forward, the liquid bridge first solidifies in the central molten pool, followed by the solidification of the rear liquid droplet. In other words, the bumps and the sunken parts intermittently or alternately appear. (f) The hump bead gradually forms after several cycles comprising step (a) – step (e). The six steps in the hump bead formation process are illustrated in Fig. 3.

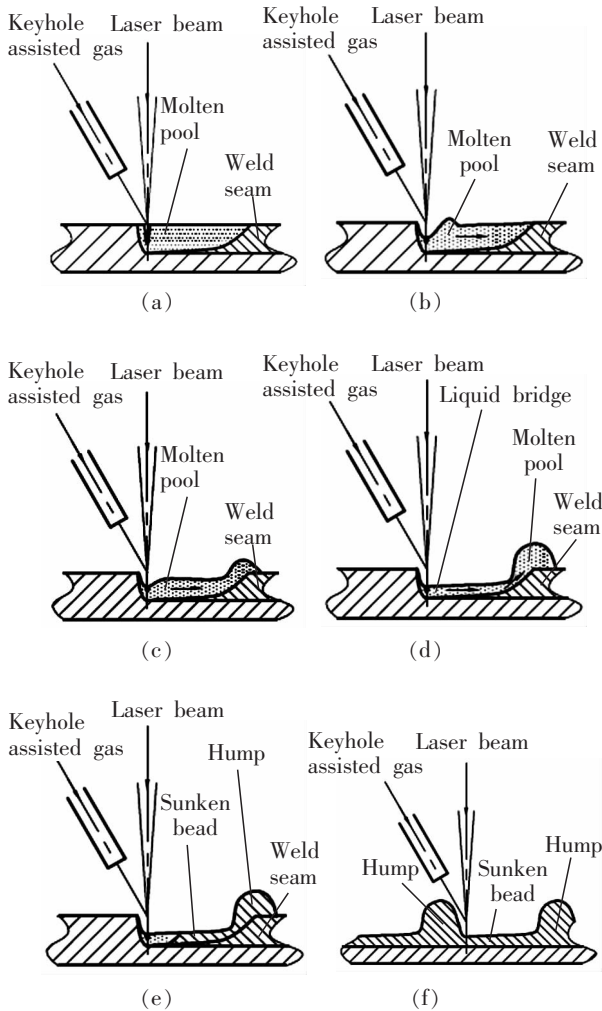


Fig. 3 Six steps of hump formation in gas-jet-assisted keyhole laser welding (shielding gas is omitted)

The main driving force for hump bead formation in laser welding is excessive gas flow. Furthermore, the key elements of hump formation lie in the premature solidifica-

tion of the rear part of the molten pool caused by large temperature gradients between the surface and the bottom of a longer molten pool, and a one-way flow of the thin-layer liquid bridge. The sequential images of the formation process of a humping weld captured by the high-speed camera corresponding to Fig. 3a – Fig. 3f are shown in Fig. 4a – Fig. 4f respectively, where a metal droplet forms

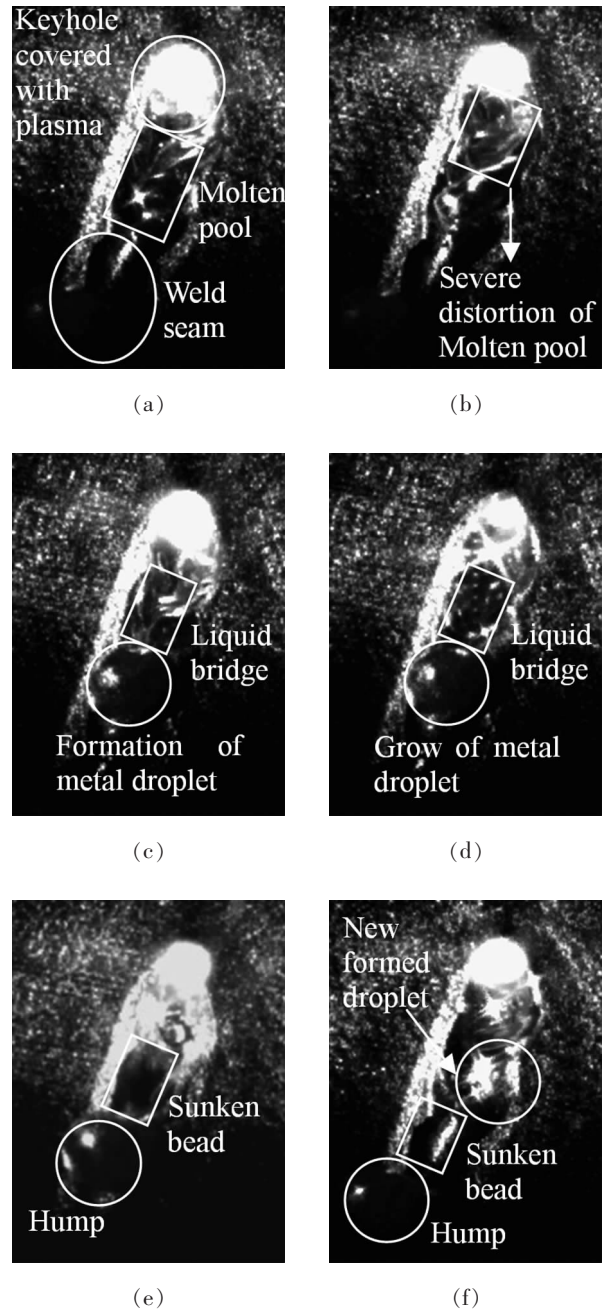


Fig. 4 Image of hump bead captured by high-speed camera (6 000 fps) in gas-jet-assisted keyhole laser welding

at the tail while the thin-layer liquid bridge is located in the middle of the molten pool between the keyhole and the droplet at the (d) step.

The formation of the hump bead in high-speed gas metal arc welding (GMAW) is attributed to two key factors^[8]: a dramatically changed force in the molten pool caused by the backward liquid flow and variation of mass distribution in the molten pool with the emergence of a thin-layer liquid metal. However, for gas-jet-assisted keyhole laser welding, under the enhanced cooling effect of excessively strong gas, the main cause of hump bead formation is the effect of large temperature gradients between the surface and the bottom of the induced thin liquid film generated by the enlarged molten pool.

4 Conclusions

(1) The weld profiles in gas-jet-assisted keyhole laser welding can be categorized into four types, welds of traditional laser welding, welds of enhanced laser welding, undercut welds, and humping welds with an increase in the gas-flow rate which is helpful for a more comprehensive understanding of the role of keyhole-assisted gas flow.

(2) The hump formation in gas-jet-assisted keyhole laser welding can be divided into six steps. The main driving force behind hump formation is the excessive large dynamic pressure of the gas jet. The following two reasons lead to the hump formation: premature solidification of the molten pool caused by the large temperature gradient between the surface and the bottom of the induced thin liquid film generated by the enlarged molten pool, and the emergence of a thin layer liquid bridge with one-directional flow under the enhanced cooling effect of excessively strong gas.

References

- [1] Kelly S M, Brown S W, Tressler J F, et al. Using hybrid laser arc welding to reduce distortion in ship panels. *Welding Journal*, 2009, 88(3): 32–36.
- [2] Zhang, X D, Ashida E, Tarasawa S, et al. Welding of thick stainless steel plates up to 50 mm with high brightness lasers. *Journal of Laser Applications*, 2011, 23(2): 807–819.
- [3] Zeng X Y, Gao M, Yan J. Effects of shielding gas in laser-arc hybrid welding. *China Journal of Lasers*, 2011, 38(6): 0601005–1–7. (in Chinese)
- [4] Chen Y B, Lei Z L, Li L Q, et al. Influence of shielding gas pressure on welding characteristics in CO₂ laser-MIG hybrid welding process. *Chinese Optics Letters*, 2006, 4(1): 33–35.
- [5] Yang J, Li X Y, Chen L, et al. Microstructure and properties of twin spot laser welded joints of 1420 Al-Li alloy. *Rare Metal Materials and Engineering*, 2011, 40(5): 871–874.
- [6] Shan J G, Zhang T, Ren J L. Influence of oxide activating fluxes on weld penetration in light beam welding. *Transactions of the China Welding Institution*, 2008, 29(2): 8–12, 88. (in Chinese)
- [7] Kamimuki K, Inoue T, Yasuda K, et al. Prevention of welding defect by side gas flow and its monitoring method in continuous wave Nd:YAG laser welding. *Journal of Laser Applications*, 2002, 14(3): 136–145.
- [8] Chen J, Wu C S. Numerical simulation of forming process of humping bead in high speed GMAW. *Acta Metallurgica Sinica*, 2009, 45(9): 1070–1076. (in Chinese)
- [9] Hess A, Dausinger F. Humping mechanisms during high-speed welding with brilliant lasers. *Proceedings of 3rd Pacific International Conference on Applications of Lasers and Optics*, Beijing, China: Laser Institute of America, 2008: 140–145.
- [10] Soderstrom E, Mendez P. Humping mechanisms present in high speed welding. *Science and Technology of Welding and Joining*, 2013, 11(5): 572–579.
- [11] Nguyen T C, Weckman D C, Johnson D A, et al. High speed fusion weld bead defects. *Science and Technology of Welding and Joining*, 2013, 11(6): 618–633.
- [12] Mills K C, Keene B J. Factors affecting variable weld penetration. *International Materials Reviews*, 1990, 35(1): 185–216.
- [13] Fabbro R, Slimani S, Doudet I, et al. Experimental study of the dynamical coupling between the induced vapour plume and the melt pool for Nd-Yag CW laser welding. *Journal of Physics D: Applied Physics*, 2006, 39(2): 394–400.
- [14] Fabbro R. Melt pool and keyhole behavior analysis for deep penetration laser welding. *Journal of Physics D: Applied Physics*, 2010, 43(44): 573–580.
- [15] Gao M, Zeng X Y, Hu Q W, et al. Mechanism and remedy of undercut formation during laser-arc hybrid welding. *Transactions of the China welding institution*, 2008, 29(6): 85–88. (in Chinese)